

- 1 **Title** (120 characters or less): Vitamin D3 regulates estrogen's action and affects mammary epithelial
- 2 organization in 3D cultures
- 3 **Short Title** (50 characters): Vitamin D3 regulates mammary epithelial organization
- 4 **Authors:** Nafis Hasan¹, Carlos Sonnenschein^{1,2}, Ana M. Soto^{1,2}
- 5 ¹Cell, Molecular & Developmental Biology Program, Sackler School of Graduate Biomedical Sciences,
- 6 Tufts University, ²Department of Immunology, Tufts University School of Medicine, Boston, MA.
- 7 **Corresponding Author** – Ana M. Soto, ana.soto@tufts.edu
- 8 **Keywords** (6) – vitamin D3, mammary gland development, epithelial organization, calcitriol, estrogen,
- 9 morphogenesis
- 10 **Disclosures** – The authors declare no competing financial interests.

11 **Abstract**

12 Vitamin D3 (vitD3) and its active metabolite, calcitriol (1,25-(OH)₂D₃), affect multiple tissue types by
13 interacting with the vitamin D receptor (VDR). Although vitD3 deficiency has been correlated with
14 increased incidence of breast cancer and less favorable outcomes across ethnic groups and latitudes,
15 randomized human clinical trials have yet to provide conclusive evidence on the efficacy of vitD3 in
16 treating and/or preventing breast cancer. When considering that carcinogenesis is “development gone
17 awry”, it becomes imperative to understand the role of vitD3 during breast development. Mammary
18 gland development in VDR KO mice is altered by increased ductal elongation and lateral branching
19 during puberty, precocious and increased alveologenesis at pregnancy and delayed post-lactational
20 involution. These developmental processes are largely influenced by mammotropic hormones, i.e.,
21 ductal elongation by estrogen, branching by progesterone and alveologenesis by prolactin. However,
22 research on vitD3’s effects on mammary gland morphogenesis focused on cell proliferation and
23 apoptosis in 2D culture models and utilized supra-physiological doses of vitD3, conditions that spare the
24 microenvironment in which morphogenesis takes place. Here, using two 3D culture models, we
25 investigated the role of vitD3 in mammary epithelial morphogenesis. We found that vitD3 interferes
26 with estrogen’s actions on T47D human breast cancer cells in 3D differently at different doses, and
27 recapitulates what is observed *in vivo*. Also, vitD3 can act autonomously and affect the organization of
28 MCF10A cells in 3D collagen matrix by influencing collagen fiber organization. Thus, we uncovered how
29 vitD3 modulates mammary tissue organization independent of its already known effects on cell
30 proliferation.

31 **Introduction**

32 Breast cancer remains a major cause of mortality among women worldwide. Epidemiological studies
33 have shown that key stages during breast development are particularly susceptible to the effects of
34 carcinogens. For instance, women aged 10-19 years who were exposed to atomic bomb radiation in
35 Hiroshima in World War II showed an excess of breast cancer cases at the age of prevalence compared
36 to similarly exposed women aged 35 years and older (1). Likewise, women exposed to diethylstilbestrol
37 during fetal life have a higher risk of breast cancer compared to unexposed women (2), and women
38 exposed to DDT in the womb showed a four-fold higher risk of breast cancer in adulthood (3). This
39 phenomenon has also been observed in rodents; namely, rats exposed to NMU around puberty have a
40 100% incidence of tumors, but the incidence rate falls to just 10% when exposed after 90 days of age (4).
41 Rodents exposed *in utero* to low doses of BPA have also shown a higher incidence of mammary gland
42 tumors in adult life (5,6). These “windows of susceptibility” coincide with key milestones of
43 organogenesis and/or tissue remodeling, buttressing the notion that carcinogenesis is “development
44 gone awry.”(7)

45 Vitamin D3 (VitD3), and its active metabolite calcitriol (1,25-(OH)₂D₃), has been primarily studied in the
46 context of normal and diseased bone development (8). However, research over the past few decades
47 have shown that vitD3 can affect multiple tissue types, including the mammary gland (8). For instance,
48 epidemiological data from human populations across different ethnicities and latitudes show a
49 correlation between vitD3 deficiency and risk of breast cancer incidence, and between vitD3 deficiency
50 and worse outcomes for breast cancer patients (8-10). Animal models show that calcitriol deficiency
51 promotes tumor growth in mice (11), and vitamin D receptor (VDR) KO animals have a higher mortality
52 rate when they are crossed into a genetically induced breast cancer model background (12). Moreover,
53 dietary supplementation of vitD3 inhibited tumor growth in xenograft models of breast and prostate
54 cancers in mice (13). Although vitD3 supplementation may help with patient outcomes, and post-

55 menopausal women may benefit from a lower breast cancer risk (14), there is yet no conclusive
56 evidence from randomized clinical trials that validates the efficiency of vitD3 as a therapeutic or
57 preventive option for breast cancer.

58 Mammary glands from VDR KO mice exhibit a florid developmental phenotype, as exemplified by
59 increased number of terminal end buds (TEBs), increased ductal extension and lateral branching at
60 puberty (15), precocious alveologensis during pregnancy, and delayed post-lactational involution (16).
61 These developmental processes are largely influenced by the so-called mammotropic hormones, i.e.,
62 Estradiol (E2), Progesterone (Prg) and Prolactin (Prl). More specifically, E2 induces ductal elongation, Prg
63 increases lateral branching and Prl stimulates alveologensis (17). The VDR KO phenotype in the
64 mammary gland of rodents indicates that vitD3 interacts with these hormones during mammary
65 epithelial morphogenesis. However, no study has yet examined the interactions between these
66 mammotropic hormones and vitD3 at these developmental stages, or explored the role of vitD3 in
67 mammary epithelial morphogenesis.

68 Studies on vitD3's action in the mammary gland have largely focused on vitD3's effects on cell
69 proliferation and apoptosis (8). These studies have mostly utilized 2D cell culture models; they do not
70 represent the 3D environment required for morphogenesis. Additionally, most studies have used a
71 calcitriol dose of 100 nM. This dose was chosen based on the deficiency cut-off level for vitD3 in human
72 populations, which is determined by measuring the serum levels of calcidiol, the precursor to calcitriol
73 (18). Therefore, utilizing such a dose assumes a hundred percent conversion rate of calcidiol to calcitriol
74 locally at specific tissues, and does not take into account that calcitriol may elicit a non-monotonic dose
75 response comparable to that observed with other steroid hormones.

76 In this study, we have utilized two different 3D cell cultures models to investigate vitD3's role in
77 mammary gland morphogenesis. We observed that calcitriol constrains E2's actions on the organization

78 of mammary epithelial cells, and that this effect is independent of its already well-characterized role in
79 cell proliferation. We also noticed that calcitriol has autonomous effects on mammary ductal
80 organization and describe a novel effect of calcitriol on the organization of collagen fibers. Finally, we
81 confirm that calcitriol elicited a non-monotonic dose response in mammary epithelial cells, as can be
82 expected from a steroid hormone, and therefore confirmed that vitD3 acts as a steroid hormone.

83 **Materials & Methods**

84 *Reagents*

85 Hydrocortisone, cholera toxin, insulin, Dulbecco's modified Eagle's medium (DMEM), Phosphate
86 Buffered Saline (PBS, 10x), and calcitriol were purchased from Sigma-Aldrich (St. Louis, MO). DMEM/F12,
87 L-Glutamine and Trypsin were purchased from Life Technologies (Carlsbad, CA). 17β -estradiol (E2) was
88 purchased from Calbiochem. Fetal bovine and equine sera were purchased from Thermo Fisher
89 (Waltham, MA). Epidermal Growth Factor (EGF) and rat tail type I collagen were purchased from Corning
90 (Tewksbury, MA). E2 and calcitriol were resuspended in ethanol to make 10^{-3} and 10^{-4} M stocks,
91 respectively.

92 *Cell maintenance*

93 Human breast epithelial T47D cells used in this study were cloned from a population originally obtained
94 from Dr. G. Green (U. Chicago). The cells used in these experiments were tested for estrogen sensitivity
95 before they were used (19). These cells were grown in the DMEM containing 5% FBS (propagation
96 medium). When looking at effects of hormones on these cells using 2D culture experiments, we used
97 DMEM/F12 without phenol red with 5% charcoal-dextran stripped FBS (CD-FBS) and 10^6 U/ml penicillin;
98 when performing 3D culture experiments with the same purpose, we used a mixture of 75% DMEM,
99 25% Ham's F12 without phenol red, 7.5% CD-FBS and 2 mM L-glutamine. Human breast epithelial
100 MCF10A cells were purchased from American Type Culture Collection (Manassas, VA) and maintained in

101 DMEM/F12 with phenol red, 5% equine serum, 20 ng/ml epidermal growth factor (EGF), 0.5 µg/ml
102 hydrocortisone, 0.1 µg/ml cholera toxin, and 10 µg/ml insulin. Experiments performed using MCF10A
103 cells used the same medium. In all cases, cells were incubated at 37°C in 6% CO₂ and 100% humidity.

104 *Dose response curves to calcitriol*

105 Dose-response curves to calcitriol in 2D culture were performed in 24-well plates. Cells were seeded at a
106 density of 35,000/well in media and allowed to attach. For MCF10A cells, seeding media was changed to
107 media containing different doses of calcitriol after 24 hours of seeding. For T47D cells, propagation
108 media was removed 48 hours after seeding, and substituted with CD-FBS medium containing different
109 doses of calcitriol with or without E2. After 6 days, cell numbers were determined using the SRB assay
110 (20).

111 *3D cultures*

112 Collagen type I gels were formulated at a final concentration of 1 mg/mL as described previously (21).
113 Cells were suspended in the gel solution at a density of 75,000 cells per gel and 1.5 mL of mixture (per
114 well) was poured into 12-well plates. The mixture was allowed to congeal for 30 min at 37°C, and 1.5 mL
115 of appropriate media was added to each well (CD-FBS media containing E2 +/- calcitriol for T47D,
116 MCF10A media +/- calcitriol). Gels were detached as previously described (22). Cultures were
117 maintained either for 1 week to measure total cell yield or 2 weeks for morphological assessments. At
118 each endpoint, gels were harvested and processed as described by Speroni et al (21). Briefly, to count
119 cell numbers, cells were extracted by digesting 3D gels with collagenase and then lysed to obtain nuclei
120 that were then counted using a Coulter Z1 particle counter (Beckman Coulter, CA). For morphological
121 assessments, gels were harvested at 2 weeks, fixed with 10% phosphate-buffered formalin, and either
122 embedded in paraffin for histological analyses or whole mounted and stained with carmine alum to
123 visualize epithelial structures.

124 *Whole mount Analysis*

125 Whole-mounted gels stained with carmine alum were imaged using a Zeiss LSM 800 confocal
126 microscope for automated morphometric analysis as described by Paulose et al (23). Briefly, $\sim 1 \text{ mm}^2$
127 area of the gel periphery was imaged to a depth of $\sim 100 \mu\text{m}$. Resulting images were stitched together
128 and analyzed using Software for Automated Analysis (SAMA) (23) and statistical analyses of
129 morphometric parameters was performed using GraphPad Prism software.

130 *Picrosirius staining*

131 Formalin-fixed, paraffin-embedded gels were sectioned using a microtome at $5\mu\text{m}$ thickness. Gel
132 sections were then rehydrated and stained with picrosirius red solution to visualize collagen fibers and
133 counter-stained with Weigert's hematoxylin as described by Junqueira et al (24). Stained sections were
134 observed under polarized light using a Zeiss Axioskop 2 Plus microscope.

135 *Real-Time PCR*

136 Gels were digested using collagenase as described above, and RNA from cells was harvested using
137 Qiagen RNeasy mini kit according to manufacturer's instructions. Gene transcripts were quantified via
138 RT-PCR using the Luna Universal One-Step RT-qPCR kit (New England Biolabs, MA) in an iQ5
139 thermocycler (Bio-rad, CA). Transcript levels were normalized to *RPL19* transcripts levels. Primer
140 sequences for genes analyzed are as follows - *PRGAB* 5'-GAGGATAGCTCTGAGTCCGAGGA-3' (forward),
141 5'-TTTGCCCTTCAGAAGCGG-3' (reverse); *RPL19* 5'-TAGTCTGGCTTCAGCTTCCTC-3' (forward), 5'-
142 TCTGCAACATCCAGCTACCC-3' (reverse); *CYP24A1* 5'-GAAAGAATTGTATGCTGCTGCACA-3'(forward), 5'-
143 GGGATTACGGGATAAATTGTAGAGAA-3' (reverse).

144 *Statistics*

145 GraphPad Prism and SPSS software were used for all statistical analyses. One-way ANOVA followed by
146 Tukey's *post hoc* test were performed to determine differences in the dose-response curves, number of
147 elongated structures in MCF10A gels and MCF10A gel diameters; one-way ANOVA with *post hoc*
148 Dunnett's 2-sided *t*-test was performed for cell yields in T47D 3D gels. Kruskal-Wallis test was performed
149 to determine differences in the morphometric parameters of structures. Chi-square analysis was
150 performed to compare distributions of T47D epithelial structures in different volume categories.
151 Unpaired *t*-test with Welch's correction was used to analyze RT-PCR data. For all statistical tests, results
152 were considered significant at $p < 0.05$.

153 **Results**

154 **Effects of calcitriol on estrogen-induced cell proliferation**

155 T47D cells exposed to different doses of vitD3 showed a decrease in cell numbers at the end of a 6-day
156 period only when in the presence of estrogen in both 2D and 3D cultures (Fig. 1). However, the reduced
157 cell yield was observed at the 50 nM and 100 nM doses of vitD3 alone in 2D (Fig. 1A), whereas a reduced
158 cell yield was observed only at the 100 nM dose in 3D (Fig. 1B). Based on our inverted microscope
159 visualization of dead "floaters" in these cultures, the decrease in cell yield, especially in 2D culture, can
160 be attributed to cell death. In contrast, we observed an increase in cell numbers at lower calcitriol doses,
161 such as 10 and 25 nM in 3D culture, a phenomenon that has not been previously reported. Separately,
162 calcitriol activity in these cells was confirmed by performing RT-PCR for *CYP24A1* gene transcripts; there
163 was a dose-dependent increase following calcitriol treatment (Supp. Fig. 1).

164 **Effects of calcitriol on Estrogen-induced epithelial organization**

165 Previous work from our lab had shown that E2 induces T47D cells to form mostly elongated shaped
166 structures when embedded in a 3D rat tail collagen type I matrix (21). Using this same model, we
167 investigated how vitD3 affects the organization of T47D cells in the presence of 0.1 nM E2. As shown in

168 Fig. 2, calcitriol affects the organization of these cells, mainly by affecting the volume of the epithelial
169 structures, in a dose-dependent manner (Supp. Fig. 2). More specifically, the change in the organization
170 is seen through a re-distribution of different sized structures in the population – the 50 nM calcitriol
171 dose results in a higher number of smaller structures whereas the 10 nM dose results in a slight, non-
172 statistically significant increased number of larger structures (Fig. 2B). In contrast, calcitriol alone does
173 not seem to affect these cells when added to the hormone-depleted CD-FBS medium, thus suggesting
174 that either the interactions with E2 are responsible for the effects observed, or the effect of calcitriol is
175 independent of E2 but is unobservable as the cells are not proliferating in the absence of E2.

176 Further investigation into vitD3's effects on epithelial organization using our unsupervised and unbiased
177 analysis revealed that calcitriol affects morphological parameters of the T47D epithelial structures, also
178 in a dose-dependent manner. The 50 nM calcitriol dose resulted in a reduction in the major radius of the
179 ellipsoid (*ell_majrad*; Fig. 3A) and an increase in the elongation ratio (*elon1*; Fig. 3B); this observation
180 suggests that this dose results in smaller and thinner structures compared to those induced by 0.1 nM
181 E2. In contrast, the 10 nM calcitriol dose resulted in a decrease in sphericity (Fig. 3C) and an increase in
182 the flatness ratio (*elon2*; Fig. 3D); in this condition, the T47D structures are more elongated and wider
183 compared to those in the E2 control.

184 **Calcitriol interferes with estrogen's transcriptional effects**

185 Previous studies have indicated that vitD3 interferes with E2-induced gene expression in cultured cells
186 and human breast tissue (25). To delineate whether vitD3 was interacting with E2's activity at the
187 transcriptional level, we performed RT-PCR to examine levels of Progesterone receptor (*PRGAB*)
188 transcripts, which are a reliable indicator of E2's activity both *in vitro* and *in vivo*. We observed that both
189 50 and 100 nM calcitriol diminished *PRGAB* induction by E2 by ~60% in T47D cells in 3D culture, as

190 shown in Fig. 4. This indicates that calcitriol interferes with E2's activity at the transcriptional level in our
191 model.

192 **Estrogen-independent effects of vitD3**

193 MCF10A cells are considered normal breast epithelial cells because they do not form tumors when
194 inoculated into nude/SCID mice (26) and form normal acinar and ductal structures in 3D cultures (27). To
195 investigate whether vitD3 has autonomous effects on mammary epithelial cell proliferation and
196 organization, we chose to investigate calcitriol's effects on MCF10A cells under those conditions.
197 MCF10A cells are ER negative; as shown by the induction of *CYP24A1* gene transcripts, they respond to
198 calcitriol in a dose-dependent manner (Supp. Fig. 3). Because calcitriol exposure resulted in lower cell
199 numbers starting at 10 nM in 3D compared to 100 nM in 2D culture, these cells appear to be more
200 sensitive to calcitriol in 3D culture conditions (Fig. 5). MCF10A cells exhibited a monotonic dose-
201 response relationship in both cases.

202 **Autonomous effects of calcitriol on epithelial organization**

203 MCF10A cells embedded in bovine type I collagen formed predominantly ductal structures with few
204 acinar structures after 2 weeks in culture (27). Using this model, we investigated vitD3's effects on the
205 organization of these cells; however, we utilized a rat tail type I collagen matrix (Fig. 6). Previous work
206 from our lab (28) has shown that epithelial organization in 3D culture is influenced by the species of the
207 collagen type I used in the extracellular matrix formulation. Consistent with those and other findings
208 (29), we observed mostly acinar structures with few ductal structures in a rat tail type I collagen matrix
209 (Fig. 6A). Interestingly, we also observed that calcitriol increases the number of elongated structures in
210 3D culture, with the highest number observed at the 10 nM dose, followed by a reduction at higher
211 doses (25 & 50 nM, Fig. 6B).

212 **Effects of calcitriol on MCF10A epithelial organization**

213 Confocal images of MCF10A 3D gels were analyzed for changes in the morphological parameters of the
214 epithelial structures upon calcitriol treatment. Exposure to calcitriol resulted in flatter and less spherical
215 structures; these effects were significant at the 50 nM dose (Fig. 7). Calcitriol also resulted in a decrease
216 in the volume of these epithelial structures, most significantly at 50 nM dose (Supp. Fig. 4), which can be
217 attributed to the increase in flatness with increasing calcitriol doses.

218 **Effects of calcitriol on collagen organization**

219 MCF10A cells organize collagen fibers in the 3D gels, as a prerequisite for organizing into ducts or acini
220 (30). Because of the changes in the morphological parameters of the epithelial structures, we
221 investigated collagen fiber organization in 3D gels using picrosirius staining. Polarized light microscopy of
222 FFPE sections stained with picrosirius revealed that calcitriol has a non-monotonic effect on collagen
223 fiber organization in this 3D model (Fig. 8). Calcitriol at 10 nM dose reduced the number of organized
224 collagen fibers. In contrast, 25 and especially 50 nM doses showed an increase in the amount of
225 organized collagen fibers. Additionally, at these doses, organized fibers were more uniformly distributed
226 throughout the 3D gels, especially in areas distal from epithelial structures (data not shown). These
227 observations may explain why calcitriol treatment also resulted in increased contraction of the 3D gels
228 in a dose-dependent manner after 2 weeks in culture (Supp. Fig. 5).

229 **Discussion**

230 Despite evidence linking vitD3 deficiency to increased risk of breast cancer and worse clinical outcomes
231 in patients, randomized clinical trials have yet to confirm the efficacy of vitD3 as a preventive or
232 therapeutic option in this disease (8). Experimentally, while VDR KO mice do not develop tumors
233 spontaneously, mammary glands from these mice exhibit a striking phenotype of excessive and
234 precocious development at key stages (15,16). This suggests that vitD3 plays an important role in the
235 development of the normal mammary gland. When considering that carcinogenesis is “development

236 gone away” (7), an understanding of the role of vitD3 in this process may provide worthy therapeutic
237 options for breast cancer patients.

238 The VDR is expressed in the mammary gland at the different stages of postnatal development that are
239 largely influenced by the mammotropic hormones E2, Prg and Prl. These hormones have well-
240 characterized effects on the morphogenesis of the gland; for example, E2 stimulates ductal elongation,
241 Prg increases lateral branching and Prl induces alveologensis (17). Although the VDR KO phenotype of
242 the gland has been described (15,16), no reference has been made so far to the interactions between
243 E2, Prg and Prl, and vitD3 in a 3D environment in which morphogenesis takes place. To fulfill this need,
244 we have utilized two different 3D culture models to tease out vitD3’s effects that are either dependent
245 or independent of its interactions with E2. We noticed that calcitriol exhibits a non-monotonic dose
246 response only in 3D cultures, a phenomenon not previously described. This is in line with current
247 knowledge regarding steroid hormone activity and also favors the notion that vitD3 functions as a
248 steroid hormone.

249 In the presence of estrogen in 3D culture, calcitriol increases total cell yield at 10 nM dose whereas it
250 decreases total cell yield at 100 nM dose (Fig. 1B). This reduction in cell yield can be attributed to cell
251 death given our observation of floater cells in both 2D and 3D cultures. Comparable evidence was found
252 when the role of vitD3 was explored in apoptosis (8,25). We also observed that calcitriol constrains the
253 effects of E2 on mammary epithelial morphogenesis without affecting total cell yield, more specifically
254 on the organization of epithelial ductal structures in 3D conditions. Consistent with our finding, the
255 mammary glands of *CYP24A1* KO mice, which cannot metabolize calcitriol, exhibit stunted development
256 (31); Zinser et al (16) report that VDR KO mammary glands exhibit increased ductal elongation at
257 puberty. Of note, in both of these models, the proliferative capacity of the epithelial cells was not
258 affected. Given that E2 is responsible for ductal elongation during puberty, our results recapitulate

259 vitD3's activity *in vivo* and confirm that calcitriol constrains the effects of estrogen on ductal elongation
260 without affecting cell death or proliferation.

261 During puberty, the mouse mammary gland epithelial ducts elongate under the influence of E2.

262 However, only 15-20% of epithelial cells in the gland are ER-positive at that time (32), with this protein
263 being expressed in the interior luminal layer of epithelial cells and not in the outermost cap layer. A
264 similar pattern of VDR expression in the mammary gland epithelium at puberty has been reported, with
265 most expression observed in the trailing edge of the terminal end buds and lesser expression in the cap
266 cells (15). Therefore, while E2 appears to directly affect 15-20% of epithelial cells during puberty, its
267 effects are observed at the tissue level.

268 In order to investigate whether vitD3 autonomously affects epithelial cells beyond its interactions with
269 E2, we utilized an estrogen-independent 3D culture model. MCF10A cells, considered to portray a
270 "normal-like" behavior *in vitro*, organize into mostly acinar and form some ductal structures in the 3D
271 collagen matrix (27). We observed that vitD3 retains its non-monotonic effects on morphogenesis even
272 in an estrogen-independent 3D culture model. We showed that this organization of MCF10A cells is
273 affected in a dose-dependent manner when treated with calcitriol in 3D cultures. These cells showed
274 greater sensitivity to calcitriol in 3D when compared to 2D cultures, with cell death increasing in a dose-
275 dependent manner upward from a 10 nM dose (Fig. 5).

276 Mechanical forces are the main mediators of shape during morphogenesis. Previously, we have shown
277 that mammary epithelial cells embedded in a type I collagen matrix manipulate the collagen fibers
278 around them in the process of organizing into complex shapes such as ducts and acini (21,30); these
279 epithelial cells exert mechanical forces that act on collagen fibers and on other cells. As fibers organize,
280 they constrain the cells on their ability to move and to proliferate (33). We have also shown that
281 hormones distinctively influence the way epithelial cells organize collagen fibers, and consequently

282 determine the shape of the structures formed (21,34). Based on these results, we hypothesized that
283 vitD3 would also affect fiber organization. MCF10A cells treated with increasing concentrations of
284 calcitriol in 3D cultures increase the contraction of gels. Treatment with calcitriol also decreased the
285 number of cells in the gels in a dose-dependent manner. Gel contraction is dependent on the number of
286 cells present in the gel and on the manipulation of collagen fibers by the cells. While the lower number
287 of cells can account for the smaller sizes of structures observed in the 3D gels treated with calcitriol, this
288 does not explain the increased contraction of these gels. Picrosirius staining revealed that even though
289 there are fewer cells in the gels at 50 nM dose, there is a more uniform distribution of organized fibers
290 throughout the gel (Fig. 8). As our lab and others (35) have described, organized fibers are responsible
291 for transmission of forces and more organization of fibers leads to increased anisotropy in the 3D
292 environment. The increased contraction of the gels can therefore be explained by the transmission of
293 forces across long distances by the cells, a phenomenon previously reported (36).

294 We also observed that at 10 nM dose of calcitriol there was the least amount of organized fibers and the
295 greatest number of elongated structures (Fig. 8). On closer observation, the calcitriol treated gels
296 contained a lower number of branched, elongated structures (ductal, tubular) and a higher number of
297 unbranched, elongated structures (cord-like). Additionally, when compared to untreated gels, increase
298 in calcitriol dose resulted in shorter and thinner elongated structures. We have previously reported that
299 MCF10A cells embedded in a collagen type I matrix form ductal/tubular structures in the periphery of
300 the gel and cord-like structures in inner areas (22). In the calcitriol treated gels, in addition to the inner
301 areas, cord-like structures were also observed in the periphery. The arrangement of collagen fibers by
302 the cells is affected by a multitude of factors that include physical constraints. Therefore, in order to
303 fully elucidate the differential organization of structures depending on the calcitriol dose used,
304 additional measurements of local biomechanical parameters in the calcitriol-treated 3D gels is required.

305 All models, by definition, are simplified versions of the object being modeled. They are used precisely
306 because they reduce the number of variables considered relevant to explain a phenotype. Thus, like all
307 experimental models, 3D culture models have their limitations. For example, the use of established cell
308 lines, which are considered rather stable is dictated by the limitations of using freshly isolated primary
309 cells. Isolated human primary cells are not efficient in forming biologically relevant structures in collagen
310 or ECM matrices *in vitro*; only a small percentage of them express mammatropic hormone receptors and
311 they lose their potential to form structures shortly after being placed in culture (37-39). Considering
312 these inherent limitations, we have utilized human breast epithelial cell lines such as T47D and MCF10A
313 to create more robust, consistent and complementary models that would still mimic the mammary
314 gland morphogenesis observed *in vivo*.

315 Future work should incorporate findings from *in vitro* 3D models and test them in an *in vivo* model. To
316 that end, findings that calcitriol constrains the action of estrogen can be incorporated into a mammary
317 gland transplant model between VDR KO and wild type animals to investigate the role of the stromal
318 and epithelial compartments in mediating vitD3's effects during pubertal development. Similarly, a fetal
319 mammary gland *ex vivo* culture model (40) can also be utilized to more comprehensively understand the
320 role of vitD3 in early development.

321 Here, we have shown that calcitriol, at physiologically relevant doses, have effects beyond cell death
322 and proliferation described in the current literature. This study highlights the role of vitD3 as a
323 morphogen to the extent that calcitriol contributes to the proper shape formation of the mammary
324 gland development. Disorganization of the tissue architecture during early developmental phases has
325 been shown to contribute to tumor formation in the mammary gland in adult life (6,41). This study
326 provided a more detailed understanding of vitD3's role in normal mouse mammary gland development
327 and a lead on how vitD3 deficiency might contribute to increased breast cancer risk.

328 **Acknowledgements**

329 We would like to thank Cheryl Schaeberle for her help with statistical analyses and a critical reading of
330 this manuscript.

331 **References**

- 332 **1.** McGregor H, Land CE, Choi K, Tokuoka S, Liu PI, Wakabayashi T, Beebe GW. Breast cancer
333 incidence among atomic bomb survivors, Hiroshima and Nagasaki, 1950-69. *JNatlCancer Inst*
334 1977; 59:799-811
- 335 **2.** Palmer JR, Wise LA, Hatch EE, Troisi R, Titus-Ernstoff L, Strohsnitter W, Kaufman R, Herbst AL,
336 Noller KL, Hyer M, Hoover RN. Prenatal diethylstilbestrol exposure and risk of breast cancer.
337 *Cancer Epidemiology, Biomarkers & Prevention* 2006; 15:1509-1514
- 338 **3.** Cohn BA, La Merrill M, Krigbaum NY, Yeh G, Park JS, Zimmermann L, Cirillo PM. DDT exposure in
339 utero and breast cancer. *Journal of Clinical Endocrinology and Metabolism* 2015; 100:2865-2872
- 340 **4.** Thompson TA, Haag JD, Gould MN. ras gene mutations are absent in NMU-induced mammary
341 carcinomas from aging rats. *Carcinogenesis* 2000; 21:1917-1922
- 342 **5.** Acevedo N, Davis B, Schaeberle CM, Sonnenschein C, Soto AM. Perinatally administered
343 Bisphenol A as a potential mammary gland carcinogen in rats. *Environ Health Perspect* 2013;
344 121:1040-1046
- 345 **6.** Vandenberg LN, Maffini MV, Schaeberle CM, Ucci AA, Sonnenschein C, Rubin BS, Soto AM.
346 Perinatal exposure to the xenoestrogen bisphenol-A induces mammary intraductal hyperplasias
347 in adult CD-1 mice. *Reproductive Toxicology* 2008; 26:210-219
- 348 **7.** Soto AM, Brisken C, Schaeberle CM, Sonnenschein C. Does cancer start in the womb? Altered
349 mammary gland development and predisposition to breast cancer due to in utero exposure to
350 endocrine disruptors. *Journal of Mammary Gland Biology and Neoplasia* 2013; 18:199-208
- 351 **8.** Feldman D, Krishnan AV, Swami S, Giovannucci E, Feldman BJ. The role of vitamin D in reducing
352 cancer risk and progression. *Nature Reviews: Cancer* 2014; 14:342-357
- 353 **9.** Estébanez N, Gómez-Acebo I, Palazuelos C, Llorca J, Dierssen-Sotos T. Vitamin D exposure and
354 risk of breast cancer: a meta-analysis. *SciReports* 2018; 8:9039
- 355 **10.** O'Brien KM, Sandler DP, Taylor JA, Weinberg CR. Serum vitamin D and risk of breast cancer
356 within five years. *Environmental Health Perspectives* 2017; 125:077004
- 357 **11.** Jeong Y, Swami S, Krishnan AV, Williams JD, Martin S, Horst RL, Albertelli MA, Feldman BJ,
358 Feldman D, Diehn M. Inhibition of mouse breast tumor-initiating cells by calcitriol and dietary
359 vitamin D. *MolCancer Ther* 2015; 14:1951-1961
- 360 **12.** Zinser GM, Welch J. Vitamin D receptor status alters mammary gland morphology and
361 tumorigenesis in MMTV-neu mice. *Carcinogenesis* 2004; 25:2361-2372
- 362 **13.** Swami S, Krishnan AV, Wang JY, Jensen K, Horst R, Albertelli MA, Feldman D. Dietary vitamin D3
363 and 1,25-dihydroxyvitamin D3 (calcitriol) exhibit equivalent anticancer activity in mouse
364 xenograft models of breast and prostate cancer. *Endocrinology* 2012; 153:2576-2587
- 365 **14.** de Sousa Almeida-Filho B, De Luca Vespoli H, Pessoa EC, Machado M, Nahas-Neto J, Nahas EAP.
366 Vitamin D deficiency is associated with poor breast cancer prognostic features in
367 postmenopausal women. *JSteroid BiochemMolBiol* 2017; 174:284-289
- 368 **15.** Zinser GM, Packman K, Welch J. Vitamin D(3) receptor ablation alters mammary gland
369 morphogenesis. *Development* 2002; 129:3067-3076

- 370 **16.** Zinser GM, Welsh J. Accelerated mammary gland development during pregnancy and delayed
371 postlactational involution in vitamin D3 receptor null mice. *Molecular Endocrinology* 2004;
372 18:2208-2223
- 373 **17.** Brisken C, O'Malley B. Hormone action in the mammary gland. *Cold Spring Harb Perspect Biol*
374 2010; 2:a003178
- 375 **18.** Hollis BW. Circulating 25-hydroxyvitamin D levels indicative of vitamin D sufficiency: implications
376 for establishing a new effective dietary intake recommendation for vitamin D. *J Nutr* 2005;
377 135:317-322
- 378 **19.** Soto AM, Sonnenschein C, Chung KL, Fernandez MF, Olea N, Olea-Serrano MF. The E-SCREEN
379 assay as a tool to identify estrogens: an update on estrogenic environmental pollutants.
380 *Environmental Health Perspectives* 1995; 103:113-122
- 381 **20.** Skehan P, Storeng R, Scudiero D, Monks A, McMahon J, Vistica D, Warren JT, Bokesch H, Kenney
382 S, Boyd MR. New colorimetric cytotoxicity assay for anticancer-drug screening. *Journal of the*
383 *National Cancer Institute* 1990; 82:1107-1112
- 384 **21.** Speroni L, Whitt GS, Xylas J, Quinn KP, Jondeau-Cabaton A, Georgakoudi I, Sonnenschein C, Soto
385 AM. Hormonal regulation of epithelial organization in a 3D breast tissue culture model. *Tissue*
386 *EngPart C Methods* 2014; 20:42-51
- 387 **22.** Dhimolea E, Maffini MV, Soto AM, Sonnenschein C. The role of collagen reorganization on
388 mammary epithelial morphogenesis in a 3D culture model. *Biomaterials* 2010; 31:3622-3630
- 389 **23.** Paulose T, Montévil M, Speroni L, Cerruti F, Sonnenschein C, Soto AM. SAMA: A method for 3D
390 morphological analysis. *PLoS ONE* 2016; 11:e0153022
- 391 **24.** Junqueira LC, Bignolas G, Brentani RR. Picrosirius staining plus polarization microscopy, a specific
392 method for collagen detection in tissue sections. *Histochemistry Journal* 1979; 11:447-455
- 393 **25.** Krishnan AV, Swami S, Feldman D. Vitamin D and breast cancer: inhibition of estrogen synthesis
394 and signaling. *J Steroid Biochem Mol Biol* 2010; 121:343-348
- 395 **26.** Soule HD, Maloney TM, Wolman SR, Peterson WD, Brenz R, McGrath CM, Russo J, Pauley RJ,
396 Jones RF, Brooks SC. Isolation and characterization of a spontaneously immortalized human
397 breast epithelial cell line, MCF-10. *Cancer Research* 1990; 50:6075-6086
- 398 **27.** Krause S, Maffini MV, Soto AM, Sonnenschein C. A novel 3D in vitro culture model to study
399 stromal-epithelial interactions in the mammary gland. *Tissue EngPart C Methods* 2008; 14:261-
400 271
- 401 **28.** Dhimolea E, Soto AM, Sonnenschein C. Breast epithelial tissue morphology is affected in 3D
402 cultures by species-specific collagen-based extracellular matrix. *J Biomed Mat Res A* 2012;
403 100:2905-2912
- 404 **29.** Sweeney MF, Sonnenschein C, Soto AM. Characterization of MCF-12A cell phenotype, response
405 to estrogens, and growth in 3D. *Cancer Cell Int* 2018; 18:43
- 406 **30.** Barnes C, Speroni L, Quinn K, Montévil M, Saetzler K, Bode-Animashaun G, McKerr G,
407 Georgakoudi I, Downes S, Sonnenschein C, Howard CV, Soto AM. From single cells to tissues:
408 interactions between the matrix and human breast cells in real time. *PLoS ONE* 2014; 9:e93325
- 409 **31.** Sheng L, Turner AG, Tarulli GA, Barratt K, Kremer R, Morris HA, Callen DF, Anderson PH.
410 Conditional inactivation of the 25-hydroxyvitamin D-24-hydroxylase (Cyp24a1) in the mouse
411 mammary epithelium alters mammary gland development. *San Antonio Breast Cancer*
412 *Symposium* 2016;
- 413 **32.** Fendrick JL, Raafat AM, Haslam SZ. Mammary gland growth and development from the
414 postnatal period to postmenopause: Ovarian steroid receptor ontogeny and regulation in the
415 mouse. *Journal of Mammary Gland Biology and Neoplasia* 1998; 3:7-22

- 416 **33.** Montévil M, Speroni L, Sonnenschein C, Soto AM. Modeling mammary organogenesis from
417 biological first principles: Cells and their physical constraints. *Progress in Biophysics and*
418 *Molecular Biology* 2016; 122:58-69
- 419 **34.** Liu Z, Speroni L, Quinn KP, Alonzo C, Pouli D, Zhang Y, Stuntz E, Sonnenschein C, Soto AM,
420 Georgakoudi I. 3D organizational mapping of collagen fibers elucidates matrix remodeling in a
421 hormone-sensitive 3D breast tissue model. *Biomaterials* 2018; 179:96-108
- 422 **35.** Schedin P, Keely PJ. Mammary gland ECM remodeling, stiffness, and mechanosignaling in
423 normal development and tumor progression. *Cold Spring HarbPerspectBiol* 2011; 3:a003228
- 424 **36.** Guo CL, Ouyang M, Yu JY, Maslov J, Price A, Shen CY. Long-range mechanical force enables self-
425 assembly of epithelial tubular patterns. *Proceedings of the National Academy of Science of the*
426 *United States of America* 2012; 109:5576-5582
- 427 **37.** Novaro V, Roskelley CD, Bissell MJ. Collagen-IV and laminin-1 regulate estrogen receptor alpha
428 expression and function in mouse mammary epithelial cells. *Journal of Cell Science* 2003;
429 116:2975-2986
- 430 **38.** Linnemann JR, Miura H, Meixner LK, Irmeler M, Kloos UJ, Hirschi B, Bartsch HS, Sass S, Beckers J,
431 Theis FJ, Gabka C, Sotlar K, Scheel CH. Quantification of regenerative potential in primary human
432 mammary epithelial cells. *Development* 2015; 142:3239-3251
- 433 **39.** Sokol ES, Miller DH, Breggia A, Spencer KC, Arendt LM, Gupta PB. Growth of human breast
434 tissues from patient cells in 3D hydrogel scaffolds. *Breast Cancer Res* 2016; 18:19
- 435 **40.** Speroni L, Voutilainen M, Mikkola ML, Klager SA, Schaeberle CM, Sonnenschein C, Soto AM. New
436 insights into fetal mammary gland morphogenesis: differential effects of natural and
437 environmental estrogens. *Scientific Reports* 2017; 7:40806
- 438 **41.** Dhimolea E, Wadia PR, Murray TJ, Settles ML, Treitman JD, Sonnenschein C, Shioda T, Soto AM.
439 Prenatal exposure to BPA alters the epigenome of the rat mammary gland and increases the
440 propensity to neoplastic development. *PLoS ONE* 2014; 9:e99800

Hasan et al. Figures

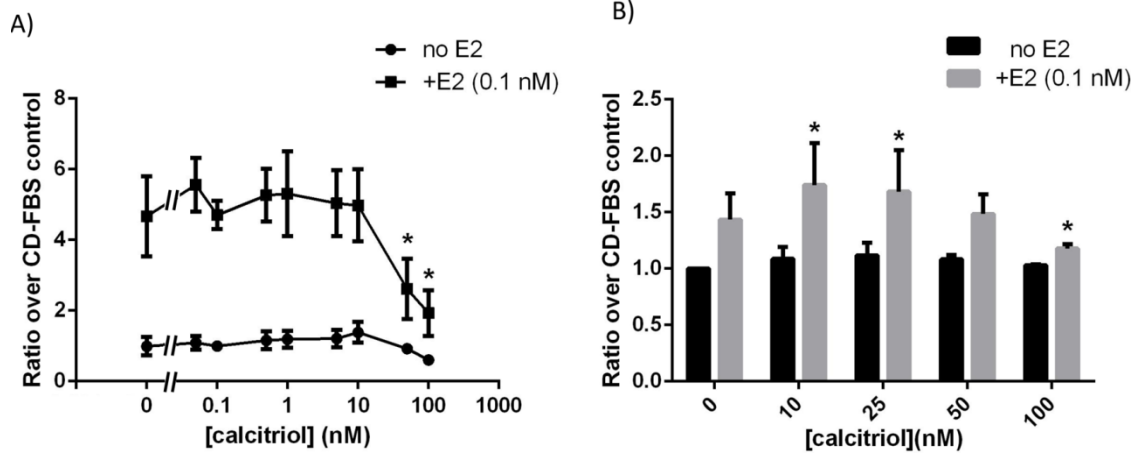


Fig. 1. Calcitriol affected total cell yield of T47D cells differently in 2D and 3D culture conditions, and only in the presence of E2 (0.1 nM). (A) Calcitriol reduced total cell yield starting at 50 nM and higher doses in 2D culture ($*p < 0.05$, one-way ANOVA). (B) Calcitriol resulted in increased cell numbers at 10 and 25 nM doses, but decreased total cell number at 100 nM dose ($*p < 0.05$ compared to E2, one-way ANOVA).

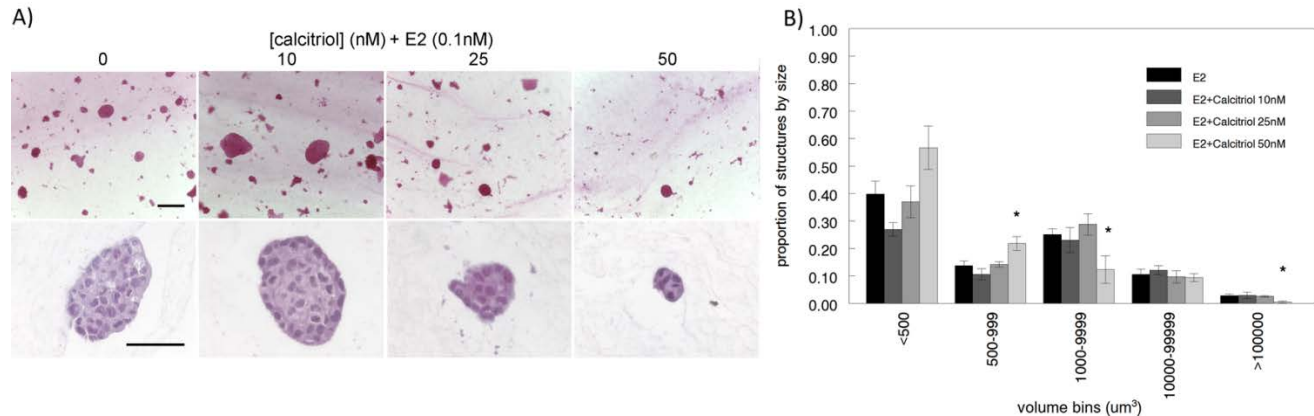


Fig. 2. Calcitriol affected the organization of T47D cells in 3D collagen matrix in the presence of 0.1 nM E2, in a dose-dependent manner. (A) Calcitriol's dose-dependent effects observed in carmine-alum stained whole mounted gels (top; scale bar=200 μm), and in H/E stained FFPE sections (bottom; scale bar=50 μm). (B) 50 nM dose resulted in an increased number of smaller structures with a concomitant decrease in larger structures ($*p < 0.05$, chi-square).

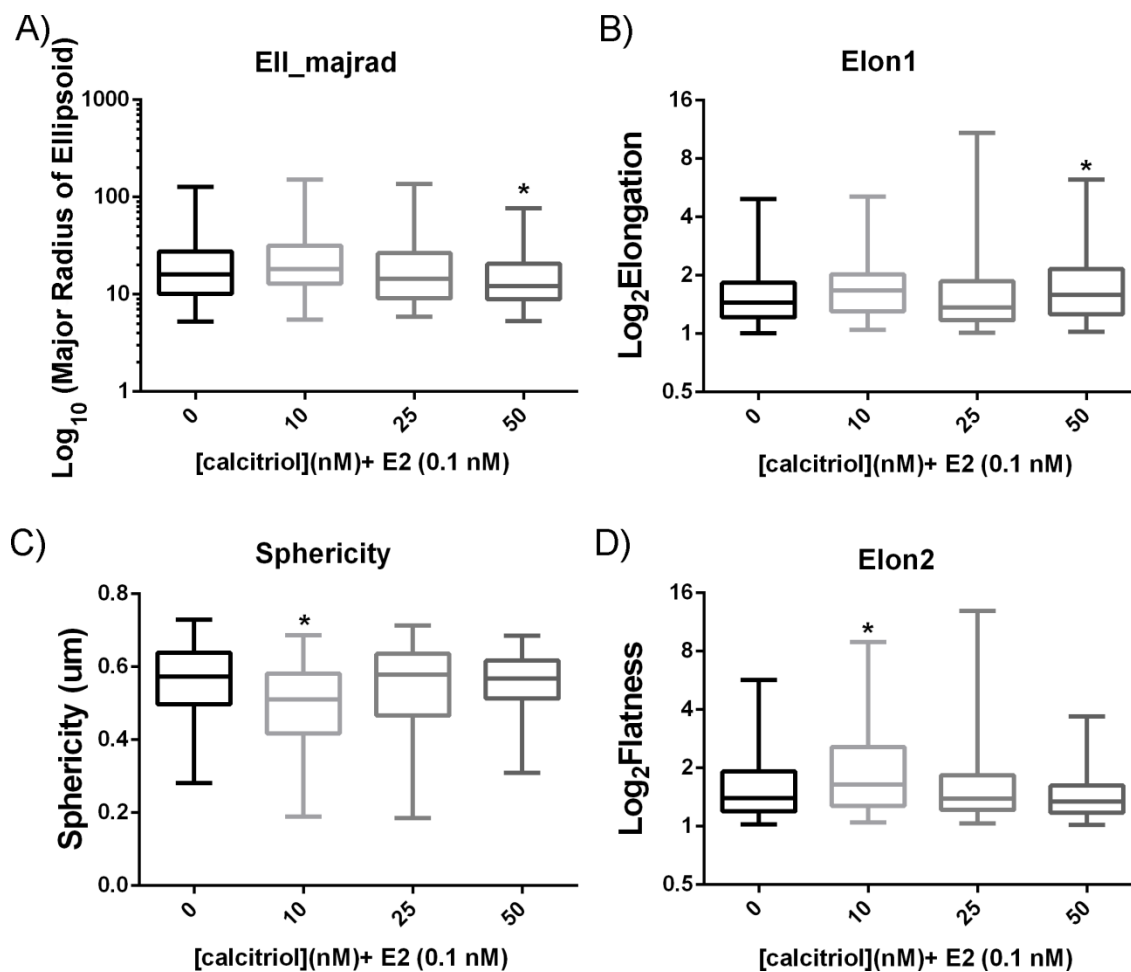


Fig. 3. Calcitriol affected physiological parameters of T47D epithelial structures in a dose-dependent manner. Compared to 0.1 nM E2 controls, 50 nM calcitriol resulted in smaller and thinner structures as shown by a decrease in the major radius of the ellipsoid (A) and an increase in the elongation ratio (B), whereas 10 nM calcitriol resulted in more elongated and wider structures as shown by a decrease in sphericity (C) and an increase in flatness ratio (D; * $p < 0.05$, Kruskal-Wallis Test.)

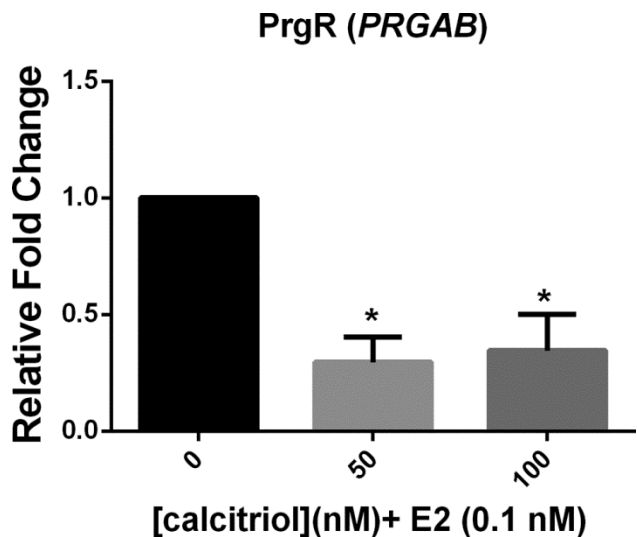


Fig. 4. Calcitriol decreased E2-induced upregulation of Progesterone receptor expression (PrgR, *PRGAB*) at both 50 and 100 nM doses (* $p < 0.05$, *t*-test). Transcripts were measured in T47D cells from 3D collagen gels after 72 hours incubation.

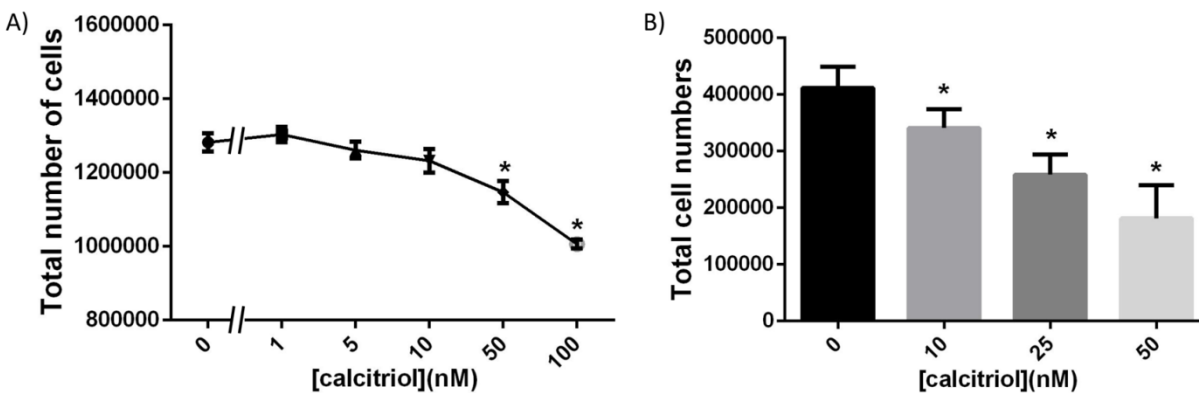


Fig. 5. MCF10A cells showed differential sensitivity to calcitriol depending on culture conditions. (A) 100 nM calcitriol significantly decreased total cell numbers in 2D culture, but in 3D culture (B), the effects were observed starting at 10 nM (* $p < 0.05$, one-way ANOVA).

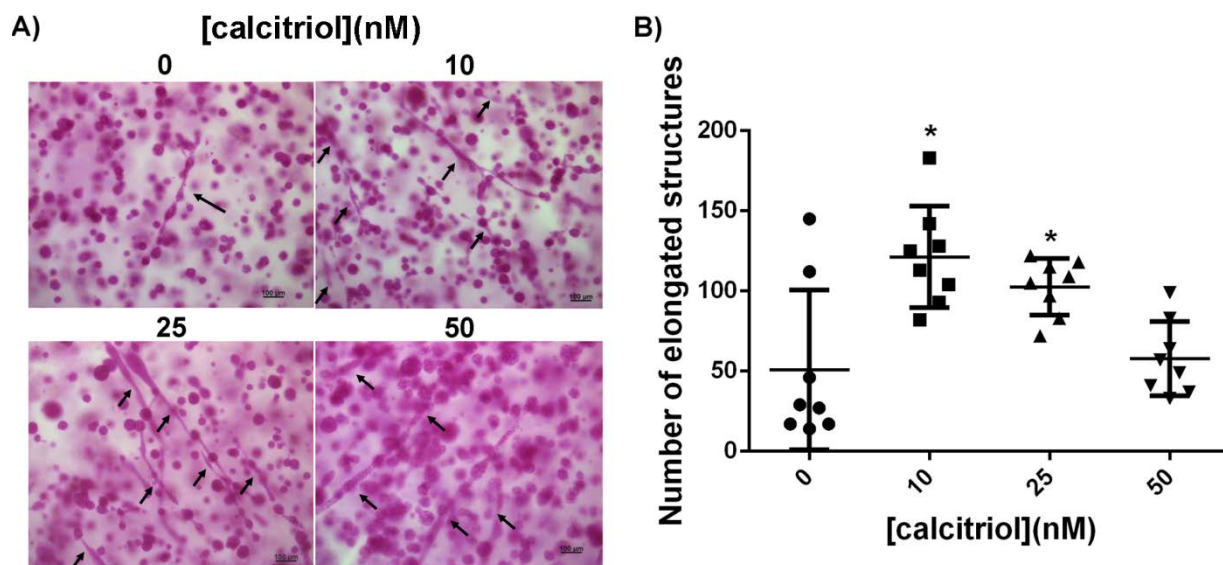


Fig. 6. Calcitriol treatment resulted in increased number of elongated structures in a non-linear fashion. (A) Carmine-alum stained whole mounts showing elongated structures (arrows; scale bar= 100 μ m). (B) Quantification of elongated structures in gels show that 10 nM calcitriol resulted in the highest number with consequent decline in higher calcitriol doses (* p <0.05, one-way ANOVA).

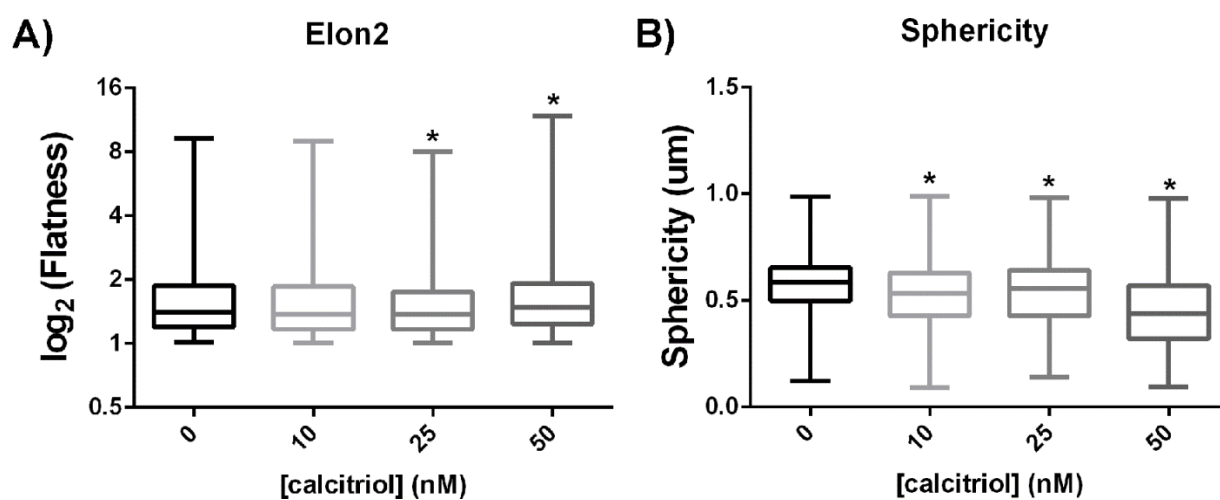


Fig. 7. Calcitriol treatment resulted in (A) flatter and (B) less spherical MCF10A epithelial structures in a type I collagen 3D matrix when cultured for 2 weeks (* p <0.05, Kruskal-Wallis.)

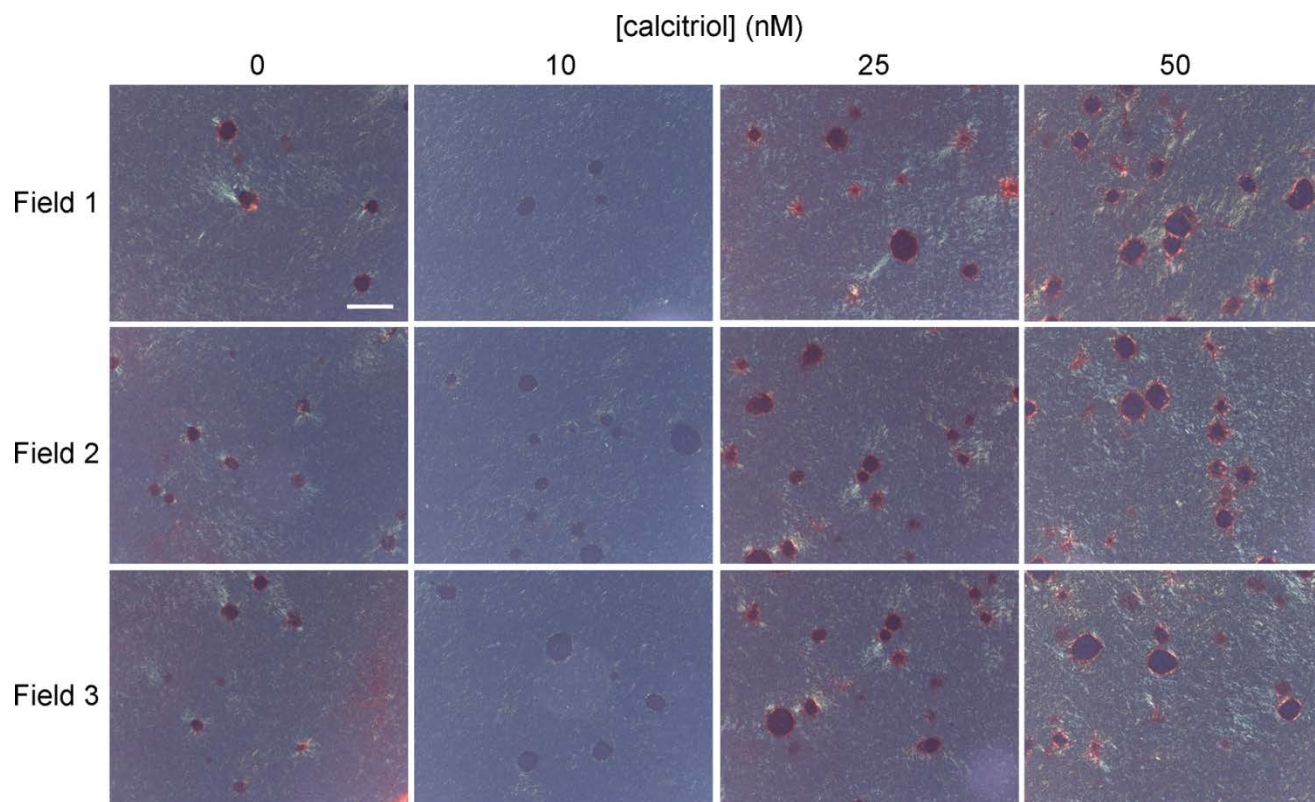


Fig. 8. Calcitriol exposure resulted in a different collagen organization in MCF10A 3D gels. See representative images from three different fields of view for each treatment group (scale bar=100 μ m)